On s-elementary wavelets in R and their applications in solving integral equations

M. J. Kheirdeh [1] *, A. Askari Hemmat[1,2,3] †, H. Saeedi[2,3] ‡
[1] Department of Mathematics,
Payame Noor University (PNU),
P.O.Box 19395-4697, Tehran, Iran.
[2] Department of Applied Mathematics,
Faculty of Mathematics and Computer,
Shahid Bahonar University of Kerman, Kerman, Iran.
[3] Mahani Mathematical Research Center,
Shahid Bahonar University of Kerman, Kerman, Iran.

Abstract

In this paper, we introduce a class of s-elementary wavelets as the basis functions and use them to present an operational computational method for solving nonlinear Fredholm and Volterra integral equations. For presenting the methods, first, operational matrices for the s-elementary wavelets are derived. Then, the s-elementary wavelets bases along with these operational matrices are applied for solving integral equations. Convergence analysis of the s- elementary wavelets basis are investigated. To reveal the accuracy and efficiency of the proposed method some numerical examples are included and the obtained results are compared with some references.

Keywords: Wavelet sets; s-elementary wavelets; Integral equations; Operational matrix.

1 Introduction

The word wavelet was first introduced by Haar in 1909 and it was developed by Chui [5], Daubechies [9], Dai and Lu [8], Meyer[22], Fang and Wang

*E-mail: kheirdeh2@gmail.com
†E-mail: askari@uk.ac.ir
‡E-mail: saeedi@uk.ac.ir

[10] and Hernandez and Weiss [14]. A special type of wavelet that is called s-elementary wavelet, first introduced by Dai and Larson [6] also, Gabardo and Yu [11] and Benedetto and Sumetkijakan [2], have come up with new and different ways to build these wavelet sets.
In recent years, integral theory has attracted much more attention from physicists and mathematicians. In fact there are many problems in physics, mechanics, chemistry and biology that are in the form of partial differential equations, linear and nonlinear integral equations. There are several methods for solving these types of equations as the polynomial approximation [28], linear multistep methods [3], modified homotopy perturbation [12, 29], wavelets [31], triangular functions [27], Newton–Kantorovich method [24] and the Haar wavelet method and the higher order Haar wavelet method [4, 15, 17, 18, 19, 20, 21, 23, 30].
In section 2, we will recall wavelets and introduce s-elementary wavelets and using them to create a suitable wavelet basis for solution of integral equations.
Section 3 is devoted to introduce s-elementary wavelets operational matrices and how to find its entries.
In section 4, we will analyse the convergence of s-elementary wavelets approximation series.
In the last section, we use of s-elementary wavelets for numerical solution of Fredholm and Volterra integral equations and compare the results with the previous methods.

2 Wavelet sets and bases

Assuming that the reader is familiar with the content of wavelet analysis. We have provided the definitions and main content of this section from references [6, 7, 14].

Definition 2.1. The function $\psi \in L^2(\mathbb{R})$ is called a 2-dilation wavelet, if the set $\{\psi_{jm}\}_{j,m\in\mathbb{Z}}$ is an orthonrmal basis for $L^2(\mathbb{R})$, here ψ_{jm} is defined by $\psi_{jm}(x) := 2^{\frac{j}{2}}\psi(2^j x - m)$.

Definition 2.2. Let $\{V_j\}_{j\in\mathbb{Z}}$ be a sequence of closed subspaces of functions in $L^2(\mathbb{R})$. The collection of spaces $\{V_j\}_{j\in\mathbb{Z}}$ is called a Multiresolution Analysis (MRA) $L^2(\mathbb{R})$ if the following conditions hold,
1. $V_j \subset V_{j+1}$ for all $j \in \mathbb{Z}$,
2. $f(.) \in V_j$ iff $f(2.) \in V_{j+1}$ for all $j \in \mathbb{Z}$,
3. $\bigcap_{j\in\mathbb{Z}} V_j = \{0\}$ and $\bigcup_{j\in\mathbb{Z}} V_j$ is dense in $L^2(\mathbb{R})$,
4. $f(.) \in V_0$ iff $f(. - n) \in V_0$ for all $n \in \mathbb{Z}$,

5. There exists a function $\varphi \in V_0$, called the **scaling function**, such that the family $\{\varphi(. - m);\ m \in \mathbb{Z}\}$ is an orthonormal basis for V_0.

Definition 2.3. If $f, g \in L^1(\mathbb{R}) \cap L^2(\mathbb{R})$ then the Fourier transform of f is defined by $\hat{f}(\xi) = \int_{-\infty}^{\infty} f(x)\, e^{-i\xi x} dx$ and the inverse Fourier transform of g by $\check{g}(x) = \frac{1}{2\pi} \int_{-\infty}^{\infty} g(\xi)\, e^{i\xi x} d\xi$.

Lemma 2.4. [14] Let φ be the scaling function of MRA and let ψ be the corresponding wavelet function. Then $|\hat{\varphi}(\xi)|^2 = \sum_{j=0}^{+\infty} |\hat{\psi}(2^j \xi)|^2$, a.e $\xi \in \mathbb{R}$.

Definition 2.5. The measurable subset $W \subset \mathbb{R}$, with finite measure, is a **wavelet set** for $L^2(\mathbb{R})$ if the inverse Fourier transform of $\hat{\psi} = \chi_W$ be an orthonrmal wavelet for $L^2(\mathbb{R})$.

Note. We are following Dai and Larson [6] and call this type of wavelets, **s-elementary wavelets**. (The prefix "s" is for "set".)

Corollary 2.6. [10] Let $W \subset \mathbb{R}$ be a measurable set and $\hat{\psi} = \chi_W$ then ψ is an orthonrmal wavelet if and only if $\{2^j W;\ j \in \mathbb{Z}\}$ and $\{W + 2\pi m;\ m \in \mathbb{Z}\}$ are both partitions of $\mathbb{R}$.

Example 2.7. In [13], it is proved that $W_c = [4\pi(c-1),\ 2\pi(c-1)) \cup (2\pi c,\ 4\pi c]$, where $c \in (0,\ 1)$, is a $2-$dilation wavelet set. For $c = 0.5$, $W_{0.5} = [-2\pi,\ -\pi) \cup (\pi,\ 2\pi]$ is the **Shannon** wavelet set.

By Lemma 2.4, the scaling function for χ_{W_c} is of the form χ_{Q_c}, with $Q_C = [2\pi(c-1),\ 2\pi c]$. Now, we put:

$$ {}_c\hat{\varphi}(x) = \begin{cases} \frac{1}{\sqrt{2\pi}}, & x \in [2\pi(c-1),\ 2\pi c], \\ 0, & \textit{other wise.} \end{cases} \tag{1} $$

Corollary 2.8. [16] If we define ${}_c\hat{\varphi}_{mk}(x) := \frac{2^{\frac{k}{2}}}{\sqrt{2\pi}}\ {}_c\hat{\varphi}\left(2^k x - 2m\pi\right)$ for $k, m \in \mathbb{Z}$ and $c \in (0,\ 1)$ where ${}_c\hat{\varphi}$ is defined as in (1), then for fix k, the system $\{{}_c\hat{\varphi}_{mk}\ ;\quad m \in \mathbb{Z}\}$ is an orthonrmal basis for $L^2(\mathbb{R})$.

By Definition 2.5 the inverse Fourier transform of χ_{W_c} is an orthonormal s-elementary wavelet. Now, we put:

$$ {}_c\hat{\psi}(x) = \begin{cases} \frac{1}{\sqrt{2\pi}}, & x \in [4\pi(c-1),\ 2\pi(c-1)) \cup (2\pi c,\ 4\pi c], \\ 0, & \textit{other wise.} \end{cases} $$

If we define ${}_c\hat{\psi}_{mk}(x) := \frac{2^{\frac{k}{2}}}{\sqrt{2\pi}}\ {}_c\hat{\psi}\left(2^k x - 2m\pi\right)$ for $k, m \in \mathbb{Z}$ and $c \in (0,\ 1)$.

In [16], the authors showed for fix k, the system $\left\{{}_c\hat{\psi}_{mk}\ ;\quad m \in \mathbb{Z}\right\}$ is an orthonrmal basis for $L^2(\mathbb{R})$.

3 S-elementary wavelets operational matrices

From now on, consider k as a fixed number unless it is mentioned as something else.

Let ${}_{(c)}\hat{\Psi}_{mk}$ be the vector of s-elementary wavelets, so we put:

$$ {}_{(c)}\hat{\Psi}_{mk} := \left[{}_c\hat{\psi}_{0k},\ {}_c\hat{\psi}_{1k},\ {}_c\hat{\psi}_{2k}, ...,\ {}_c\hat{\psi}_{mk} \right]^T. \tag{2} $$

As a consequence of definition (2), we can obtain appropriate approximation of functions in $L^2[0,1]$, if we choose k large enough. Also using large k's one can cover the interval $[0,1]$ with the union of supports of ${}_c\hat{\psi}_{mk}$'s i. e. $V = \cup_{i=0}^{m}\ supp\left({}_c\hat{\psi}_{ik}\right)$ so that the measure of $V \backslash [0,1]$ be smaller than every $\epsilon > 0$. Then for $f \in L^2[0,1]$, we have:

$$ f \simeq \sum_{i=0}^{m} d_{ik}\ {}_c\hat{\psi}_{ik} = D^T\, {}_{(c)}\hat{\Psi}_{mk}, \tag{3} $$

where $d_{ik} = \left\langle f,\ {}_c\hat{\psi}_{ik} \right\rangle$, $D^T = [d_{0k}, d_{1k}, ..., d_{mk}]$ and $\langle .,\ . \rangle$ is an inner product on $L^2[0,1]$.

Lemma 3.1. [16] Let ${}_{(c)}\hat{\Psi}_{mk}$ is the vector of s-elementary wavelets in (2). The integration of its entries can be expanded as follows,

$$ \int_0^x {}_{(c)}\hat{\Psi}_{mk}(t)\, dt = {}_{(c)}\hat{P}\ {}_{(c)}\hat{\Psi}_{mk}(x), \tag{4} $$

where the $(m+1) \times (m+1)$ matrix ${}_{(c)}\hat{P} = [{}_{(c)}\hat{p}_{ij}]$ is called the operational matrix of s-elementary wavelets and its entries are:

$$ {}_{(c)}\hat{p}_{ij} = \left\langle \int_0^{(.)} {}_c\hat{\psi}_{i-1,k}(t)dt,\ {}_c\hat{\psi}_{j-1,k} \right\rangle. $$

For $a = \frac{\pi}{2^k}$, the $(m+1)\times(m+1)$ operational matrix of s-elementary wavelets is as the following,

${}_{(c)}\hat{P}^k_{(m+1)} =$

$$ \begin{bmatrix} a & a(2c^2-2c+2) & 2a & ... & 2a & 2a \\ 2a(c-c^2) & a & a(2c^2-2c+2) & 2a & ... & 2a \\ 0 & 2a(c-c^2) & a & a(2c^2-2c+2) & ... & 2a \\ \vdots & \ddots & \ddots & \ddots & \ddots & \vdots \\ 0 & \cdots & 2a(c-c^2) & a & a(2c^2-2c+2) & 2a \\ 0 & 0 & \cdots & 0 & 2a(c-c^2) & a \end{bmatrix}. $$

For $c = 0.5$ and $m = 4$, the above matrix takes the following form,

$$ {}_{(0.5)}\hat{P}^{k}_{(5)} = \begin{bmatrix} a & \frac{3a}{2} & 2a & 2a & 2a \\ \frac{a}{2} & a & \frac{3a}{2} & 2a & 2a \\ 0 & \frac{a}{2} & a & \frac{3a}{2} & 2a \\ 0 & 0 & \frac{a}{2} & a & \frac{3a}{2} \\ 0 & 0 & 0 & \frac{a}{2} & a \end{bmatrix}_{(5\times 5)} . $$

We put:

$$ {}_{(c)}\hat{\Phi}_{mk} = \left[{}_{c}\hat{\varphi}_{0k},\ {}_{c}\hat{\varphi}_{1k},\ {}_{c}\hat{\varphi}_{2k}, ...,\ {}_{c}\hat{\varphi}_{mk} \right]^{T}, \tag{5} $$

similar to the description in the second paragraph at the beginning of this section, for $f \in L^2[0,1]$, we have:

$$ f \simeq \sum_{i=0}^{m} h_{ik}\ {}_{c}\hat{\varphi}_{ik} = H^{T}\ {}_{(c)}\hat{\Phi}_{mk}, \tag{6} $$

where $h_{ik} = \langle f,\ {}_{c}\hat{\varphi}_{ik} \rangle$, $H^T = [h_{0k}, h_{1k}, ..., h_{mk}]$.

Lemma 3.2. [16] Let ${}_{(c)}\hat{\Phi}_{mk}$ is the vector of s-elementary wavelets in (5). The integration of its entries can be expanded as follows,

$$ \int_{0}^{x} {}_{(c)}\hat{\Phi}_{mk}(t)\, dt = {}_{(c)}\hat{Q}\ {}_{c}\hat{\Phi}_{mk}(x), \tag{7} $$

where the $(m+1) \times (m+1)$ matrix ${}_{(c)}\hat{Q} = [{}_{(c)}\hat{q}_{ij}]$ is called the operational matrix of s-elementary wavelets and its entries are:

$$ {}_{(c)}\hat{q}_{ij} = \left\langle \int_{0}^{(.)} {}_{c}\hat{\varphi}_{i-1,k}(t)dt,\ {}_{c}\hat{\varphi}_{j-1,k} \right\rangle . $$

We put $a = \frac{\pi}{2^k}$, the $(m+1) \times (m+1)$ operational matrix of s-elementary wavelets is as the following:

$$ {}_{(c)}\hat{Q}^{k}_{(m+1)} = \begin{bmatrix} a & 2a & \cdots & 2a & 2a \\ 0 & a & 2a & \cdots & 2a \\ \vdots & \ddots & \ddots & \ddots & \vdots \\ 0 & \cdots & \ddots & a & 2a \\ 0 & 0 & \cdots & 0 & a \end{bmatrix}_{(m+1)\times(m+1)} . $$

Lemma 3.3. Let $E = [e_0, e_1, ..., e_m]^T$ be a vector and $\omega = \frac{2^{\frac{k}{2}}}{\sqrt{2\pi}}$. Then we have the following relationships:

$$ E^{T}\ {}_{(c)}\hat{\Psi}_{mk}\ {}_{(c)}\hat{\Psi}^{T}_{mk} = {}_{(c)}\hat{\Psi}^{T}_{mk} diag(\omega E), \tag{8} $$

$$\int_0^1 {}_{(c)}\hat{\Psi}_{mk}(x)dx = \frac{1}{\omega}[1,1,\cdots,1]^T_{(m+1)\times 1}, \tag{9}$$

$$E^T\ {}_{(c)}\hat{\Phi}_{mk}\ {}_{(c)}\hat{\Phi}^T_{mk} = {}_{(c)}\hat{\Phi}^T_{mk} diag(\omega E), \tag{10}$$

$$\int_0^1 {}_{(c)}\hat{\Phi}_{mk}(x)dx = \frac{1}{\omega}[1,1,\cdots,1]^T_{(m+1)\times 1}. \tag{11}$$

Proof. It is easy to prove it. □

4 Convergence analysis

Theorem 4.1. Let $\sum_{i=0}^{\infty} d_{ik}\ {}_c\hat{\psi}_{ik}$ be the s-elementary wavelets series of $f \in L^2[0,1]$, then $f_m = \sum_{i=0}^{m} d_{ik}\ {}_c\hat{\psi}_{ik}$ convergences to f as $m \to +\infty$.

Proof. By using relation (3), we have:

$$d_{ik} = \left\langle f,\ {}_c\hat{\psi}_{ik} \right\rangle. \tag{12}$$

First we will show that the sequence of partial sums $\sum_{i=0}^{\infty} d_{ik}\ {}_c\hat{\psi}_{ik}$, f_m, is a Cauchy sequence in the Hilbert space of $L^2[0,1]$. Let f_m be an arbitrary partial sums of $\sum_{i=0}^{\infty} d_{ik}\ {}_c\hat{\psi}_{ik}$, i.e., $f_m = \sum_{i=0}^{m} d_{ik}\ {}_c\hat{\psi}_{ik}$, also $p > m$, then we get:

$$\begin{aligned}
||f_m - f_p||^2 &= \left|\left| \sum_{i=m+1}^{p} d_{ik}\ {}_c\hat{\psi}_{ik} \right|\right|^2 \\
&= \left\langle \sum_{i=m+1}^{p} d_{ik}\ {}_c\hat{\psi}_{ik},\ \sum_{j=m+1}^{p} d_{jk}\ {}_c\hat{\psi}_{jk} \right\rangle \\
&= \sum_{i=m+1}^{p}\sum_{j=m+1}^{p} d_{ik}d_{jk} \left\langle {}_c\hat{\psi}_{ik},\ {}_c\hat{\psi}_{jk} \right\rangle \\
&= \sum_{i=m+1}^{p} |d_{ik}|^2 .
\end{aligned}$$

By Bessel'inequality, we have:

$$\sum_{i=m+1}^{p} |d_{ik}|^2 \le \sum_{i=0}^{\infty} |d_{ik}|^2 \le ||f||^2 < \infty.$$

Thus, $||f_m - f_p||^2 \to 0$ as m,p $\to +\infty$, that is, f_m is a Cauchy sequence, hence f_m converges to some $g \in L^2[0,1]$. Finally we show that $g = f$. For k

large enough and by using relation (12) and property of continuity of inner product, we get:

$$\begin{aligned}\left\langle g-f,\ {}_c\hat{\psi}_{ik}\right\rangle &= \left\langle g,\ {}_c\hat{\psi}_{ik}\right\rangle - \left\langle f,\ {}_c\hat{\psi}_{ik}\right\rangle \\ &= \lim_{m\to+\infty}\left\langle f_m,\ {}_c\hat{\psi}_{ik}\right\rangle - d_{ik} \\ &= d_{ik}-d_{ik} \\ &= 0,\end{aligned}$$

hence $g=f$ and the proof is completed. □

Note that, the above theorem is correct for $\sum_{i=0}^{\infty} h_{ik}\ {}_c\hat{\varphi}_{ik}$.

5 Application of S-elementary wavelets for solving integral equations

In this section, we present an operational method for solving a class of nonlinear Fredholm and Volterra integral equations by using the s-elementary wavelets as an application of them.
If u is the exact solution of an integral equation, fix k and consider $u_k = \sum_{i=0}^{m} d_{ik}\ {}_c\hat{\psi}_{ik}$ as the approximate solution. Then the experimental rate of convergence, $R_k(x)$, can be estimated as follows:

$$R_k(x) = \log\left|\frac{u_{k+1}(x)-u(x)}{u_k(x)-u(x)}\right|, \qquad \text{for} \qquad k=1,\ 2,\ 3,\ldots\ .$$

Remark. For different values of c, the error rate is not so significant. Table 2 shows changing c will give better accuracy for some x values and less accuracy for some other values. But in general, increasing the value of k, for a fixed c, increases the accurate.

5.1 Numerical solution of Fredholm integral equations

Consider the following nonlinear Fredholm integral equation of the second kind,

$$u(t) = f(t) + \int_0^1 K(t,s)\sum_{l=0}^{N} f_l(s)u^l(s)ds, \quad N>1, \tag{13}$$

where the functions $f, f_l \in L^2[0,1]$ and $K(t,s) \in L^2([0,1]\times[0,1])$ are given functions, $u(t)$ is unknown function and N is a positive integer. Note that in Eq. (13), for $N=1$ the equation is linear and otherwise nonlinear, which are given in examples (5.1) and (5.2). Here, we suppose that $K(t,s)=k_1(t)k_2(s)$. By Eq. (3) we get:

$$f \simeq F^T{}_{(c)}\hat{\Psi}_{mk},\ f_l \simeq F_l^T{}_{(c)}\hat{\Psi}_{mk},\ k_1 \simeq K_1^T{}_{(c)}\hat{\Psi}_{mk},$$

$$k_2 \simeq K_2^T{}_{(c)}\hat{\Psi}_{mk},\ h \simeq H^T{}_{(c)}\hat{\Psi}_{mk},\ u \simeq U^T{}_{(c)}\hat{\Psi}_{mk}. \tag{14}$$

By substitute Eqs. (14) into (13) and by Eq. (8) we have:

$$\begin{aligned}
&U^T{}_{(c)}\hat{\Psi}_{mk}(t) = F^T{}_{(c)}\hat{\Psi}_{mk}(t) + \\
&\int_0^1 K_1^T{}_{(c)}\hat{\Psi}_{mk}(t) K_2^T{}_{(c)}\hat{\Psi}_{mk}(s) \sum_{l=0}^N F_l^T{}_{(c)}\hat{\Psi}_{mk}(s) \Big(U^T{}_{(c)}\hat{\Psi}_{mk}(s)\Big)^l (s) ds \\
&= F^T{}_{(c)}\hat{\Psi}_{mk}(t) + \\
&\int_0^1 K_1^T{}_{(c)}\hat{\Psi}_{mk}(t) K_2^T{}_{(c)}\hat{\Psi}_{mk}(s) \sum_{l=0}^N F_l^T{}_{(c)}\hat{\Psi}_{mk}(s)_{(c)}\hat{\Psi}^T_{mk}(s)\ diag\left(\omega^{l-1}\ U^{l-1}\right) U ds \\
&= F^T{}_{(c)}\hat{\Psi}_{mk}(t) + \\
&\int_0^1 K_1^T{}_{(c)}\hat{\Psi}_{mk}(t) K_2^T{}_{(c)}\hat{\Psi}_{mk}(s) \sum_{l=0}^N {}_{(c)}\hat{\Psi}^T_{mk}(s)\ diag\left(\omega F_l\right)\ diag\left(\omega^{l-1}\ U^{l-1}\right) U ds \\
&= F^T{}_{(c)}\hat{\Psi}_{mk}(t) + \\
&\int_0^1 K_1^T{}_{(c)}\hat{\Psi}_{mk}(t) \sum_{l=0}^N {}_{(c)}\hat{\Psi}^T_{mk}(s)\ diag\left(\omega K_2\right)\ diag\left(\omega F_l\right)\ diag\left(\omega^{l-1}\ U^{l-1}\right) U ds \\
&= F^T{}_{(c)}\hat{\Psi}_{mk}(t) + {}_{(c)}\hat{\Psi}_{mk}(t) K_1^T \times \\
&\int_0^1 \Big(\sum_{l=0}^N {}_{(c)}\hat{\Psi}^T_{mk}(s)\ diag\left(\omega K_2\right)\ diag\left(\omega F_l\right)\ diag\left(\omega^{l-1}\ U^{l-1}\right) U\Big) ds.
\end{aligned}$$

Now, by taking transpose on both sides of above equation, we get:

$$\begin{aligned}
&{}_{(c)}\hat{\Psi}^T_{mk}(t) U = {}_{(c)}\hat{\Psi}^T_{mk}(t) F + {}_{(c)}\hat{\Psi}^T_{mk}(t) K_1 \times \\
&\Big(\sum_{l=0}^N U^T\ diag\left(\omega K_2\right)\ diag\left(\omega F_l\right)\ diag\left(\omega^{l-1}\ U^{l-1}\right) U\Big) \int_0^1 {}_{(c)}\hat{\Psi}_{mk}(s) ds \\
&U = F + K_1 \times \\
&\Big(\sum_{l=0}^N U^T\ diag\left(\omega K_2\right)\ diag\left(\omega F_l\right)\ diag\left(\omega^{l-1}\ U^{l-1}\right) U\Big) \int_0^1 {}_{(c)}\hat{\Psi}_{mk}(s) ds \\
&U = F + K_1 \times \\
&\left(\sum_{l=0}^N U^T\ diag\left(\omega K_2\right)\ diag\left(\omega F_l\right)\ diag\left(\omega^{l-1}\ U^{l-1}\right) U\right)\ \frac{1}{\omega}\ [1, 1, \cdots, 1]^T.
\end{aligned} \tag{15}$$

Eq. (15) is a system of nonlinear algebraic equations, with unknown vector U. We solve this nonlinear system by the Newton method and obtain u as $u \simeq U^T{}_{(c)}\hat{\Psi}_{mk}$. Note that the above method can be stated by basis vector (5).

Example 5.1. Consider the following nonlinear Fredholm equation [24, 25],

$$u(t) = sin(\pi t) + \frac{1}{5}\int_0^1 cos(\pi t)sin(\pi s)u^3(s)ds, \tag{16}$$

the exact solution of this equation is $u(t) = sin(\pi t) + \frac{1}{3}(20 - \sqrt{391})cos(\pi t)$. In Table 1, we compare our error approximations with the methods in [24, 25] and in Table 2, we did it for different values of c. Fig. 1, (a) and (b) show the comparisons between the approximate solutions and exact solutions, when we used ${}_{(c)}\hat{\Phi}_{mk}$ and ${}_{(c)}\hat{\Psi}_{mk}$ in our method, respectively.

Table 1: Absolute error comparison of the present method with the methods in [24, 25] (Example: 5.1).

x	[24]	[25] $N = 16$	New method by ${}_{(0.5)}\hat{\Psi}_{m,16}(x)$	New method by ${}_{(0.5)}\hat{\Phi}_{m,16}(x)$
0.1	4.74×10^{-2}	1.94×10^{-4}	2.68×10^{-4}	1.07×10^{-5}
0.2	4.03×10^{-2}	2.15×10^{-2}	2.12×10^{-4}	1.79×10^{-5}
0.3	2.93×10^{-2}	5.63×10^{-4}	1.41×10^{-4}	1.81×10^{-5}
0.4	1.54×10^{-2}	1.26×10^{-3}	6.05×10^{-5}	1.09×10^{-5}
0.5	0	1.32×10^{-3}	1.85×10^{-5}	4.30×10^{-6}
0.6	1.54×10^{-2}	1.23×10^{-3}	8.86×10^{-5}	2.61×10^{-5}
0.7	2.93×10^{-2}	3.08×10^{-4}	1.43×10^{-4}	5.18×10^{-5}
0.8	4.03×10^{-2}	1.39×10^{-3}	1.79×10^{-4}	7.79×10^{-5}
0.9	4.74×10^{-2}	4.96×10^{-5}	1.93×10^{-4}	1.001×10^{-4}

Table 2: Absolute error comparison of the present method for different values of c (Example: 5.1).

x	${}_{c}\hat{\Psi}_{m,10}(x)$ $c = 0.11$	${}_{c}\hat{\Psi}_{m,10}(x)$ $c = 0.99$	${}_{c}\hat{\Phi}_{m,10}(x)$ $c = 0.3$	${}_{c}\hat{\Phi}_{m,10}(x)$ $c = 0.8$
0.1	9.52×10^{-3}	3.54×10^{-3}	8.93×10^{-3}	2.62×10^{-5}
0.2	3.45×10^{-3}	1.46×10^{-3}	2.99×10^{-3}	1.03×10^{-2}
0.3	6.58×10^{-4}	4.06×10^{-3}	9.61×10^{-4}	4.09×10^{-3}
0.4	6.59×10^{-3}	1.36×10^{-3}	1.83×10^{-3}	4.82×10^{-4}
0.5	5.75×10^{-4}	2.99×10^{-5}	8.95×10^{-4}	2.50×10^{-4}
0.6	3.97×10^{-4}	2.08×10^{-3}	1.21×10^{-4}	3.83×10^{-3}
0.7	3.07×10^{-3}	5.21×10^{-3}	3.51×10^{-3}	2.72×10^{-3}
0.8	3.48×10^{-3}	1.92×10^{-3}	9.51×10^{-3}	1.31×10^{-3}
0.9	2.92×10^{-3}	3.39×10^{-3}	2.29×10^{-3}	1.17×10^{-2}

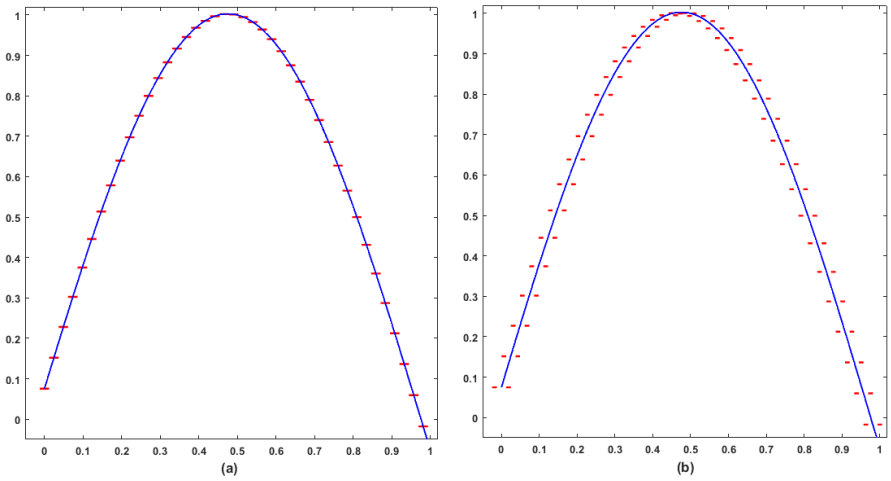

Figure 1: Comparison of the approximated solution (dashed red line) using ${}_{(0.5)}\hat{\Phi}_{m,8}$ and ${}_{(0.5)}\hat{\Psi}_{m,8}$ with the exact solution (blue line) (Example: 5.1).

Example 5.2. Consider the following nonlinear Fredholm equation [1, 24],

$$u(t) + \int_0^1 e^{t-2s} u^3(s) ds = e^{t+1}, \tag{17}$$

the exact solution of this equation is $u(t) = e^t$. In Table 3, we compare our error approximations with the methods in [1, 24] and in Table 4, we compute the rate of convergence for some k. Fig 2, (a) and (b) show the comparisons between the approximate solutions and exact solutions, when we used ${}_{(c)}\hat{\Phi}_{mk}$ and ${}_{(c)}\hat{\Psi}_{mk}$ in our method, respectively.

5.2 Numerical solution for nonlinear Volterra integral equations

Consider the following nonlinear Volterra integral equation of the second kind,

$$u(t) = f(t) + \int_0^t K(t,s) \sum_{l=0}^{N} f_l(s) u^l(s) ds, \quad N > 1, \tag{18}$$

where the functions $f, f_l \in L^2[0,1]$ and $K(t,s) \in L^2([0,1] \times [0,1])$ are given functions, $u(t)$ is unknown function and N is a positive integer. Here, we suppose that $K(t,s) = k_1(t)k_2(s)$. The proof is the same as the proof before Example 5.1, except that in the last equations according to the relation (4) we have,

Table 3: Absolute error comparison of the present method with the methods in [1, 24] (Example: 5.2).

x	[1]	[24] $N = 16$	New method by ${}_{(0.3)}\hat{\Psi}_{i,16}(x)$	New method by ${}_{(0.3)}\hat{\Phi}_{i,16}(x)$
0.1	2.05×10^{-3}	4.31×10^{-4}	8.77×10^{-5}	1.81×10^{-5}
0.2	3.30×10^{-3}	3.32×10^{-7}	9.25×10^{-5}	2.42×10^{-5}
0.3	8.69×10^{-3}	7.91×10^{-4}	9.73×10^{-5}	3.21×10^{-5}
0.4	1.69×10^{-2}	2.92×10^{-4}	1.02×10^{-4}	4.09×10^{-5}
0.5	1.87×10^{-2}	1.29×10^{-3}	1.06×10^{-4}	5.12×10^{-5}
0.6	1.17×10^{-2}	7.11×10^{-4}	1.11×10^{-4}	6.32×10^{-5}
0.7	2.93×10^{-3}	5.49×10^{-7}	1.15×10^{-4}	7.71×10^{-5}
0.8	8.08×10^{-3}	1.30×10^{-3}	1.02×10^{-4}	9.33×10^{-5}
0.9	2.16×10^{-2}	4.81×10^{-4}	1.23×10^{-4}	1.12×10^{-4}

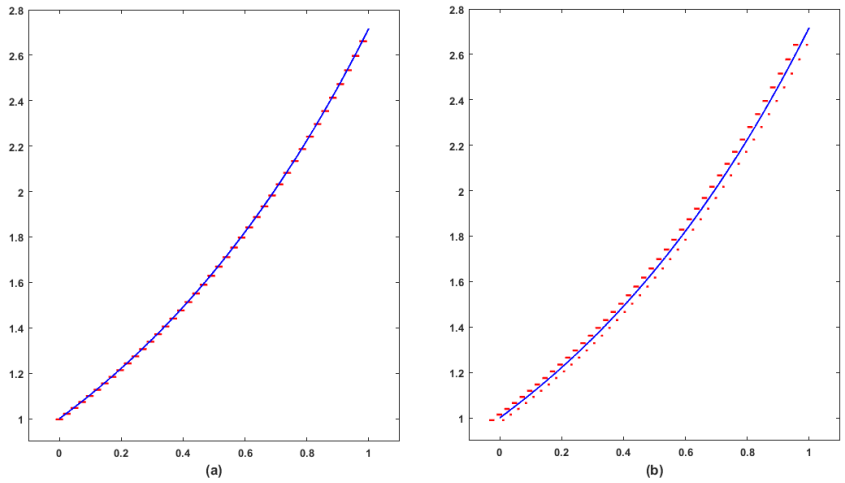

Figure 2: Comparison of the approximated solution (dashed red line) using ${}_{(0.3)}\hat{\Phi}_{m,8}$ and ${}_{(0.3)}\hat{\Psi}_{m,8}$ with the exact solution (blue line) (Example: 5.2).

$$X^T {}_{(c)}\hat{\Psi}_{mk}(t) = F^T {}_{(c)}\hat{\Psi}_{mk}(t) +$$

$$\int_0^t K_1^T {}_{(c)}\hat{\Psi}_{mk}(t) \sum_{l=0}^{N} {}_{(c)}\hat{\Psi}_{mk}{}^T(s)\ diag\,(\omega K_2)\ diag\,(\omega F_l)\ diag\left(\omega^{l-1}\ X^{l-1}\right)\ X ds$$

$$= F^T {}_{(c)}\hat{\Psi}_{mk}(t) + \left(\int_0^t K_1^T {}_{(c)}\hat{\Psi}_{mk}(t) {}_{(c)}\hat{\Psi}_{mk}^T(s) ds\right) \times \left(\sum_{l=0}^{N} diag\,(\omega K_2)\ diag\,(\omega F_l)\ diag\left(\omega^{l-1}\ X^{l-1}\right)\ X\right)$$

$$= F^T {}_{(c)}\hat{\Psi}_{mk}(t) + \left(K_1^T {}_{(c)}\hat{\Psi}_{mk}(t) {}_{(c)}\hat{\Psi}_{mk}^T(t) {}_{(c)}\hat{P}_{(m+1)}^T\right) \times$$

Table 4: Rate of convergence for (Example: 5.2).

x	$R_8(x)$	$R_{10}(x)$	$R_{12}(x)$	$R_{14}(x)$	$R_{16}(x)$
0.1	1.0804	1.0191	1.0148	1	1
0.2	1.0388	1.0073	0.9989	1	1
0.3	1.0256	1.0173	1.0007	1	1
0.4	1.0191	1.0089	1.0007	1	1
0.5	1.0152	0.9997	1.0004	1	1
0.6	1.0135	0.9969	1.0027	1	1
0.7	1.0102	1.0018	0.9996	1	1
0.8	1.0137	1.0023	1.0003	1	1
0.9	1.0163	1.0027	1.0002	1	1

$$\left(\sum_{l=0}^{N} diag\,(\omega K_2)\ \ diag\,(\omega F_l)\ \ diag\left(\omega^{l-1}\ X^{l-1}\right)\ \ X\right)$$

$${}_{(c)}\hat{\Psi}^{T}_{mk}(t)X = {}_{(c)}\hat{\Psi}^{T}_{mk}(t)F + \left({}_{(c)}\hat{\Psi}^{T}_{mk}(t)\ diag\,(\omega K_1)\ {}_{(c)}\hat{P}^{T}_{(m+1)}\right)\times$$
$$\left(\sum_{l=0}^{N} diag\,(\omega K_2)\ \ diag\,(\omega F_l)\ \ diag\left(\omega^{l-1}\ X^{l-1}\right)\ \ X\right)$$

$$X = F + \left(diag\,(\omega K_2)\ {}_{(c)}\hat{P}^{T}_{(m+1)}\right)\times$$
$$\left(\sum_{l=0}^{N} diag\,(\omega K_2)\ \ diag\,(\omega F_l)\ \ diag\left(\omega^{l-1}\ X^{l-1}\right)\ \ X\right), \tag{19}$$

Eq. (19) is a system of nonlinear algebraic equations, with unknown vector U. We solve this nonlinear system by the Newton method and obtain u as $u \simeq U^{T}{}_{(c)}\hat{\Psi}_{mk}$. Note that the above method can be stated by basis vector (5).

Example 5.3. Consider the following nonlinear Volterra equation [24, 25],

$$u(t) - \int_0^t u^2(s)ds = sin(t) - \frac{t}{2} + \frac{1}{4}sin(2t), \tag{20}$$

the exact solution of this equation is $u(t) = sin(t)$. In Table 5, we compare our error approximations with the methods in [24, 25]. Fig. 3, (a) and (b) show the comparisons between the approximate solutions and exact solutions, when we used ${}_{(c)}\hat{\Phi}_{mk}$ and ${}_{(c)}\hat{\Psi}_{mk}$ in our method, respectively.

Example 5.4. Consider the following nonlinear Volterra equation [25, 26],

$$u(t) + \int_0^t \left(u^2(s) + u(s)\right) ds = \frac{3}{2} - \frac{1}{2}e^{-2t}, \tag{21}$$

Table 5: Absolute error comparison of the present method with the methods in [24, 25] (Example: 5.3).

x	[24]	[25] $N = 16$	New method by ${}_{(0.7)}\hat{\Psi}_{m,13}(x)$	New method by ${}_{(0.7)}\hat{\Phi}_{m,13}(x)$
0.1	3.33×10^{-4}	4.40×10^{-4}	4.73×10^{-4}	2.89×10^{-4}
0.2	1.54×10^{-3}	2.79×10^{-6}	5.70×10^{-4}	1.80×10^{-4}
0.3	6.65×10^{-3}	4.69×10^{-4}	6.30×10^{-4}	1.01×10^{-4}
0.4	1.39×10^{-2}	7.69×10^{-4}	3.66×10^{-4}	3.39×10^{-4}
0.5	0.00×10^{-2}	7.31×10^{-4}	6.04×10^{-4}	6.82×10^{-5}
0.6	4.70×10^{-2}	7.68×10^{-5}	4.56×10^{-4}	1.76×10^{-4}
0.7	6.90×10^{-2}	1.84×10^{-4}	3.86×10^{-4}	2.00×10^{-4}
0.8	9.59×10^{-2}	6.48×10^{-4}	5.13×10^{-4}	2.06×10^{-5}
0.9	1.43×10^{-1}	6.68×10^{-4}	2.75×10^{-4}	2.01×10^{-4}

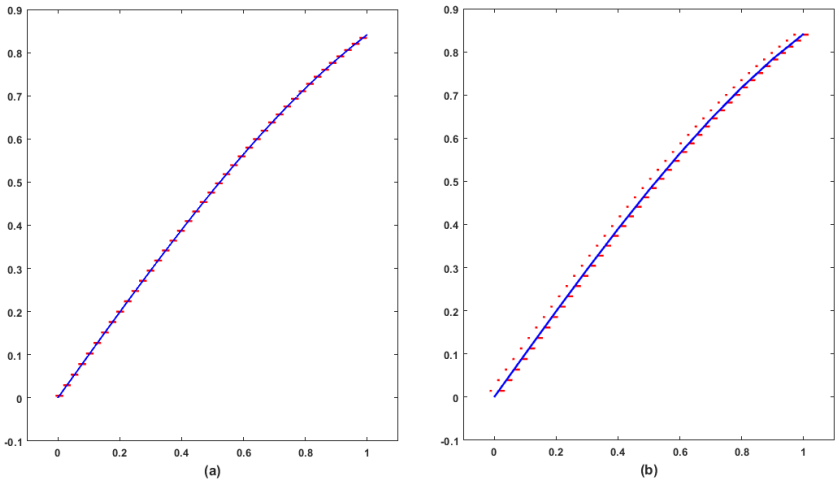

Figure 3: Comparison of the approximated solution (dashed red line) using ${}_{(0.7)}\hat{\Phi}_{m,8}$ and ${}_{(0.7)}\hat{\Psi}_{m,8}$ with the exact solution (blue line) (Example: 5.3).

the exact solution of this equation is $u(t) = e^{-t}$. In Table 6, we compare our error approximations with the methods in [25, 26] and in Table 7, we compute the rate of convergence for some k. Fig. 4, (a) and (b) show the comparisons between the approximate solutions and exact solutions, when we used ${}_{(c)}\hat{\Phi}_{mk}$ and ${}_{(c)}\hat{\Psi}_{mk}$ in our method, respectively.

Table 6: Absolute error comparison of the present method with the methods in [25, 26] (Example: 5.4).

x	[26]	[25] $N = 16$	New method by ${}_{(0.5)}\hat{\Psi}_{m,16}(x)$	New method by ${}_{(0.5)}\hat{\Phi}_{m,16}(x)$
0.1	8.33×10^{-4}	2.33×10^{-4}	1.55×10^{-4}	6.84×10^{-5}
0.2	3.75×10^{-4}	1.28×10^{-5}	1.27×10^{-4}	4.86×10^{-5}
0.3	1.11×10^{-3}	4.25×10^{-4}	1.05×10^{-4}	3.42×10^{-5}
0.4	3.51×10^{-4}	3.64×10^{-7}	8.87×10^{-5}	2.35×10^{-5}
0.5	5.80×10^{-4}	1.19×10^{-4}	7.36×10^{-5}	1.54×10^{-5}
0.6	1.32×10^{-4}	7.97×10^{-6}	6.20×10^{-5}	9.40×10^{-6}
0.7	4.95×10^{-4}	2.41×10^{-4}	5.24×10^{-5}	4.79×10^{-6}
0.8	1.73×10^{-4}	2.74×10^{-5}	4.44×10^{-5}	1.28×10^{-6}
0.9	3.68×10^{-4}	2.56×10^{-4}	3.76×10^{-5}	1.41×10^{-6}

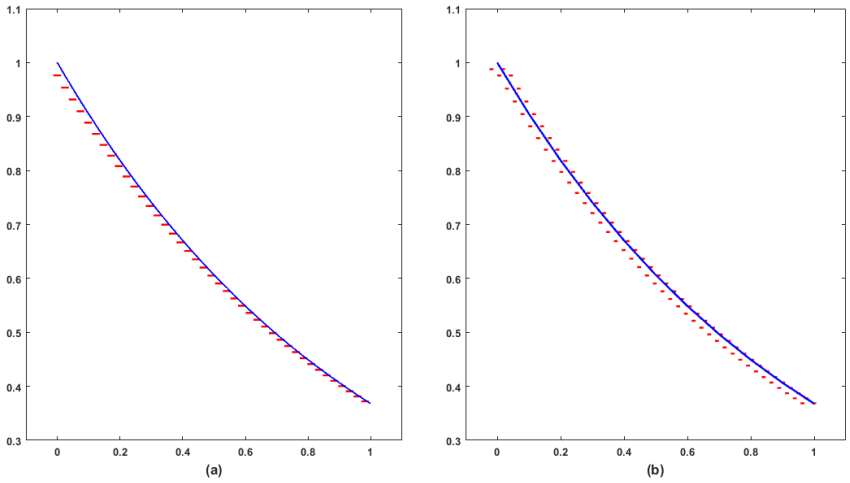

Figure 4: Comparison of the approximated solution (dashed red line) using ${}_{(0.5)}\hat{\Phi}_{m,8}$ and ${}_{(0.5)}\hat{\Psi}_{m,8}$ with the exact solution (blue line) (Example: 5.4).

6 Conclusion

In this paper we used s-elementary wavelets to solve Fredholm and Volterra integral equations. By comparing tables and figures, one can see simplicity and high accuracy of the presented basis. Also, we have a new and faster way for calculations in solving the equations mentioned in mathematics, physics and other fields.

Table 7: Rate of convergence for (Example: 5.4).

x	$R_8(x)$	$R_{10}(x)$	$R_{12}(x)$	$R_{14}(x)$	$R_{16}(x)$
0.1	0.9418	0.9537	0.9731	1	1
0.2	0.8778	1.0091	0.9947	1	1
0.3	0.9570	1.0083	0.9969	1	1
0.4	0.9710	0.9775	1.0018	1	1
0.5	0.9791	0.9833	0.9986	1	1
0.6	0.9877	0.9959	0.9964	1	1
0.7	1.0224	0.9968	0.9993	1	1
0.8	1.0206	0.9982	0.9937	1	1
0.9	1.0153	1.0038	1.0008	1	1

References

[1] E. Babolian, A. Shahsavaran: Numerical solution of nonnliniear Fredholm integral equations of the second kind using Haar Wavelets, J. Comput. Appl. Math. **225** (2009) 87-95.

[2] J. J. Benedetto and S. Sumetkijakan: A fractal set constructed from class of wavelet sets, Inverse Problems, Image Analysis, and Medical Imaging, Contemp. Math. Amer. Math Soc. Providence, RI. **313** (2002), 19-35.

[3] G. Capobianco, D. Conte, I. Del Prete: High performance parallel numerical methods for Volterra equations with weakly singular kernels. J. Comput. Appl. Math. **228** (2009), 571–579.

[4] C. F. Chen, C. H. Hsiao: Haar wavelet method for solving umped and distributed-parameter system. IEEE Proc. Control Theory Appl. **144** (1997), 87-94.

[5] C. K. Chui: An Introduction to Wavelets. Academic Press, New York, (1992).

[6] X. Dai and D. R. Larson: Wandering vectors for unitary systems and orthogonal wavelets, Amer. Math. Soc. **640** (1998).

[7] X. Dai, D. R. Larson, and D. M. Speegle: Wavelet sets in $\mathbb{R}^n$ II, Wavelets, Multiwavlets and Their Application, Contempt, Math. Amer. Math. Soc. Providence, RI. **216** (1998), 15-40.

[8] x. Dai, and S. Lu: Wavelets in subspaces. Mich. J. Math. 43 (1996), 81-98.

[9] I. Daubechies: Ten Lectures on Wavelets. CBMS 61, SIAM, (1992).

[10] X. Fang and X. Wang: Construction of minimally- supported-frequencies wavelets, J. Four. Anal. Appl. **2** (1996), 315-327.

[11] J. P. Gabardo and X. Yu: Construction of wavelet sets with certain self-similarity properties, J. Geom. Anal. **14** (2004), 629–651.

[12] A. Golbabai, B. Keramati: Solution of non-linear Fredholm integral equations of the first kind using modified homotopy perturbation method, Chaos Solit. Frac. **39** (2009), 2316-2321.

[13] E. Hernandez, X. Wang, and G. Weiss: Smoothing minimally supported frequency (MSF) wavelets: Part II. The J. Four. Anal. Appl. **2** (1995), 329–340.

[14] E. Hernandez and G. Weiss: A First course on wavelets, CRC Press, Boca Raton, FL (1996).

[15] S. U. Islam, I. Aziz, A. S. Al-Fhaid: An improved method based on Haar wavelets for numerical solution of nonlinear integral and integro-differential equations of first and higher orders, J. Comput and Appl Math. **260** (2014), 449–469.

[16] M. J. Kheirdeh, A. Askari Hemmat, H. saeedi, An application of s-elementary wavelets in solving differential and fractional integral equations numerically, J. Mahani Math. Res. Cent. 11(3) (2022) 15-31.

[17] Ü. Lepik: Haar wavelet method for nonlinear integro-differential equations, J. Math and Comput. **176** (2006), 324–333.

[18] Ü. Lepik: Application of the Haar wavelet transform to solving integral and differential equations, of the Estonian academy of sciences. Physics, Math. **56** (2007), 28–46.

[19] Ü. Lepik, H. Hein: Haar wavelets with applications, Springer, Berlin, (2014).

[20] J. Majak, M. Pohlak, K. Karjust, M. Eerme, J. Kurnitski, B. S. Shvartsman: New higher order Haar wavelet method: Application to FGM structures. Composite Structures. **201** (2018), 72-78.

[21] J. Majak, B. Shvartsman, M. Ratas, D. Bassir, M. Pohlak, K. Karjust, M. Eerme: Higher-order Haar wavelet method for vibration analysis of nanobeams, J. Materials Today Communications. **25** (2020), 101290.

[22] Y. Meyer: Wavelets and Operators, Cambridge Studies in Advanced Mathematics, **37** (1992).

[23] M. Ratas, A. Salupere, J. Majak: Solving nonlinear PDEs using the higher order Haar wavelet method on nonuniform and adaptive grids, Math Modelling and Anal. **26** (2021), 147–169.

[24] J. Saberi-Nadjafi, M. Heidari: Solving nonlinear integral equations in the Urysohn form by Newton-Kantorovich-quadrature method, Comput. Appl. Math. **60** (2010), 2058-2065.

[25] M. H. A. Sathar, A. F. N. Rasedee, A. A. Ahmedov, and N. Bachok: Numerical Solution of Nonlinear Fredholm and Volterra Integrals by Newton–Kantorovich and Haar Wavelets Methods, Symm. **12** (2020), 2034.

[26] M. Sabzevari: A review on numerical solution of nonlinear Volterra-Fredholm integral equations using hybrid of..., Alexandria Eng. J. **58** (2019), 1099-1102.

[27] H. Saeedi, G. N. Chuev: Triangular functions for operational matrix of nonlinear fractional Volterra integral equations, J. Appl. Math and Comput. **49** (2015), 213-232.

[28] F. Salehi, H. Saeedi, M. M. Moghadam: A Hahn computational operational method for variable order fractional mobile–immobile advection–dispersion equation, J. Math. Sc. **12** (2018), 91-101.

[29] H. Saeedi, F. Samimi: He's Homotop Perturbation Method for Nonlinear Ferdholm Integro-Differential Equations Of Fractional Order, Int. J. Eng. Res. Appl. **5** (2012), 52-56.

[30] M. Sorrenti, M. Di. Sciuva, J. Majak, F. Auriemma: Static Response and Buckling Loads of Multilayered Composite Beams Using the Refined Zigzag Theory and Higher-Order Haar Wavelet Method, Mechanics of Composite Materials. **57** (2021), 1-18.

[31] S. A. Yousefi, M. Razzaghi: Legendre wavelets method for the nonlinear Volterra–Fredholm integral equations, Math. Comput. Simul. **70** (2005), 1–8.